

TING HAO\*<sup>#</sup>, HAIYIN TANG\*, WEIBIN JIANG\*, XIANPING WANG\*, QIANFENG FANG\*

## MECHANICAL SPECTROSCOPY OF EQUAL-CHANNEL ANGULAR PRESSED Fe-Cr ALLOYS AND TUNGSTEN

### SPEKTROSKOPIA MECHANICZNA STOPÓW Fe-Cr I WOLFRAMU WYCISKANYCH PRZEZ KANAŁ KĄTOWY

Internal friction technique was used to investigate the microstructural stability of equal-channel angular pressed (ECAP) 9Cr1Mo steel (T91), Fe-18wt.%Cr alloy, and pure W. Several non-relaxation internal friction peaks are observed in three ECAP-strained specimens, which are related to the microstructural transition from a severely deformed state to a static recovery state of dislocations, and to recrystallized state. Along with the disappearance of the  $P_1$  peak, another relaxation internal friction peak  $P_2$  is observed during the second heating run only in Fe-18wt.%Cr alloy, and it does not disappear even during subsequent third heating run. This peak is not observed in T91 steel and W. The  $P_2$  peak is likely associated with a process of grain boundary (GB) sliding. Unlike T91, no abundant carbide precipitates distribute on GBs to pin GB and repulse GB sliding, thus, the  $P_2$  peak only occurs in Fe-18wt.%Cr alloy. It is concluded that high-temperature internal friction measurements are required to detect the grain boundary peak in pure W.

*Keywords:* Ultrafine-grained metal, equal-channel angular pressing ECAP, severe plastic deformation, Fe-Cr alloy, T91 steel, tungsten, internal friction, mechanical spectroscopy

Technika tarcia wewnętrznego została użyta do zbadania stabilności mikrostruktury poddanych wyciskaniu przez kanał kątowy stali 9Cr1Mo (T91), stopu Fe-18wt%Cr, i czystego W. Zaobserwowano wiele nie-relaksacyjnych pików tarcia wewnętrznego w trzech próbkach odkształconych przez ECAP, które są związane z przejściem ze stanu silnie odkształconego do statycznego stanu zdrowienia dyslokacji, i do stanu zrekrystalizowanego. Wraz z zanikiem pików  $P_1$ , tylko w przypadku stopu Fe-18wt%Cr obserwowany jest inny pik  $P_2$  relaksacji tarcia wewnętrznego podczas drugiego ogrzewania, i nie znika nawet w kolejnym trzecim etapie ogrzewania. Pik ten nie jest obserwowany w stali T91 i W. Pik  $P_2$  prawdopodobnie związany jest procesem poślizgu granicy ziaren. W przeciwieństwie do stali T91, brak bogatych w węgiel wydzielań na granicach ziaren, które by unieruchomiły granice i uniemożliwiły poślizg, stąd pik  $P_2$  występuje tylko w przypadku stopu Fe-18wt.%Cr. Stwierdzono, że pomiary tarcia wewnętrznego w wysokiej temperaturze są potrzebne, aby wykryć pik granicy ziarna w czystym W.

## 1. Introduction

The metallic materials with a fine grain size reveal very good mechanical properties such as higher tensile strength. However, for vast majority of commercial bulky metals and alloys, the minimum mean grain size could be obtained to be only around 10  $\mu\text{m}$  [1]. Severe plastic deformation (SPD) is a well-known method to produce ultrafine grained (UFG) and nanostructure (NS) metallic materials [2]. The equal-channel angular pressing (ECAP) is an important technique, which can produce a fine grain size in bulk materials in the ultra-fine scale and the nanometer scale [3]. The ECAP technique is successfully used to produce a variety of materials such as Cu [4], Mg [5], Fe [6], W [7], 7075 Al alloy [8], low carbon steel [9], Eurofer 97 steel [10], Al-Mg [11], etc.

One of the primary limitations of the UFG and NS materials is the thermally structural instability. When

the UFG or NS materials are heated up to some extent of temperature, the recovery and recrystallization phenomena will take place. Thus, excellent mechanical properties acquired during the SPD processing will disappear. In general, the introduction of higher strain into a crystal lattice due to SPD processing gives rise to an increase in lattice distortion elastic energy as well as the driving force of recrystallization, which is responsible for a decrease in the recrystallization temperature. This is why it is important to clarify the microstructure evolution of the UFG and NS materials during heating.

In this study, the microstructural stability of equal-channel angular pressed ferritic/martensitic 9Cr1Mo steel (T91), ferritic Fe-18wt.%Cr alloy and pure W with ultrafine grain size is investigated by mechanical spectroscopy [12-19]. Internal friction (IF) peaks are measured in the ECAP-strained samples, and their mechanisms are discussed.

\* KEY LABORATORY OF MATERIALS PHYSICS, INSTITUTE OF SOLID STATE PHYSICS, CHINESE ACADEMY OF SCIENCES, P. O. BOX 1129, HEFEI 230031, CHINA

<sup>#</sup> Corresponding author: hao.ting@issp.ac.cn

## 2. Experimental details

For the T91 steel (with compositions, in wt.%, 8.63% Cr, 0.23% Ni, 0.95% Mo, 0.43% Mn, 0.003% Ti, 0.21% V, 0.09% Nb, 0.046% Cu, 0.1% C, 0.31% Si, 0.02% P, 0.006% S, and 0.03% N), and Fe-18wt.%Cr alloy (17.88% Cr, 0.0164% Mn, 0.0532% Al, 0.003% C, 0.0014% N, 0.0041% P, 0.0048% S, 0.0383% Si, and 0.0124% O), the specimens were machined to cylindrical rods with 10 mm in diameter and 60 mm in length. Following this, the samples were put into the home-designed ECAP die with an inner contact angle ( $\varphi$ ) of  $90^\circ$  and the curvature arc of  $20^\circ$  at the outer point of contact ( $\psi$ ) to perform the ECAP processing at room temperature. All of the ECAP extrusions were carried out in route C, that is, after each extrusion the sample was rotated by  $180^\circ$  around the extrusion direction before the next extrusion.

Tungsten rods (99.9% in purity) with a diameter 10 mm and a length 30 mm were purchased from Zhuzhou Cemented Carbide Group, Co. Ltd. in China. These rods were extruded up to three passes in the home-designed ECAP die with  $\varphi = 120^\circ$  and  $\psi = 30^\circ$ . The schematic diagram of the ECAP die used in this study is described in [20]. The specimen billets and the ECAP die were simultaneously heated to either  $800^\circ\text{C}$  or  $950^\circ\text{C}$  within 2.5 h in a flowing Ar atmosphere, and then the ECAP extrusions were carried out after half hour annealing. The extrusion rate was lower than 3 mm/s.

Internal friction measurements were performed in a forced inverted torsion pendulum during ascending temperature with the heating rate of  $2^\circ\text{C}/\text{min}$  and descending temperature with the cooling rate of  $2^\circ\text{C}/\text{min}$ . The excitation frequency was in the range from 0.5 to 4 Hz. The maximum strain amplitude was  $2 \times 10^{-5}$ . To investigate thermal stability of internal friction peaks, mechanical loss measurements were repeated in the second and third heating runs.

## 3. Results and discussion

### 3.1 The P1 peak in T91 steel

Figure 1(a) shows typical internal friction spectra measured at the excitation frequency 4.0 Hz for the as-received, 1 pass, and 4 passes T91 steel specimens, respectively. No IF peak is detected in the as-received specimen. However, an asymmetrical peak is observed at about  $693^\circ\text{C}$  and  $676^\circ\text{C}$  during the first run for 1 pass and 4 passes specimens. The highest temperature during internal friction measurements was  $820^\circ\text{C}$ . These IF peaks almost disappear during the second heating run. As the peak temperature does not shift with the oscillation frequency while the peak height decreases with the increasing oscillation frequency, this internal friction peak indicates a non-relaxation feature. Similar measurements of the peak were carried out in T91 steel samples with different extrusion numbers [21]. It was demonstrated that the peak temperature shifts toward lower temperature with increasing the extrusion number [21]. Therefore, the thermal stability of ECAP-strained T91 steel decreases with strain accumulation. This peak is associated with recrystallization of T91 steel samples. It is well known that an increase in the deformation degree decreases the temperature of recrystallization beginning in the steels.

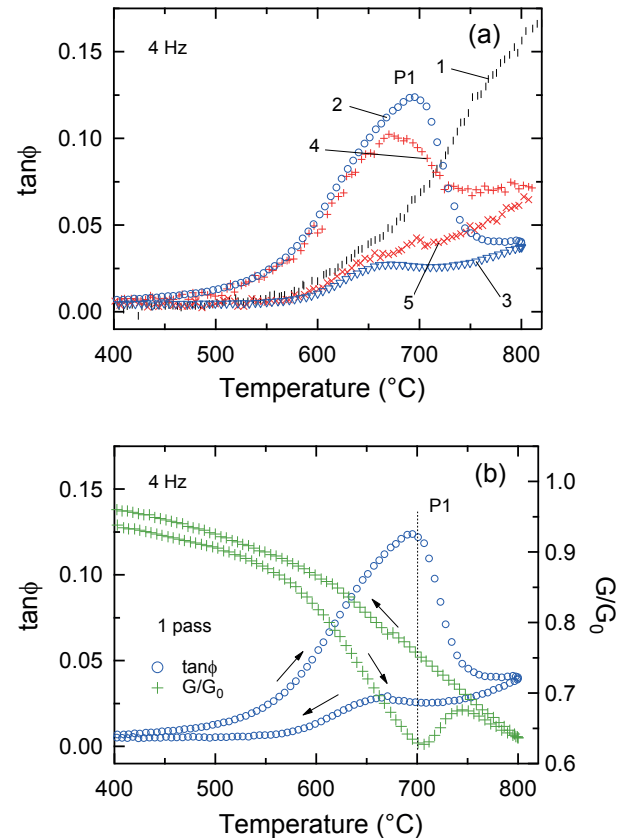


Fig. 1. (a) Internal friction spectra for the as-received T91 steel (curve 1) in the first heating and for 1 pass (curves 2-3) and 4 passes (curves 4-5) specimens in the first and second heating, (b) internal friction spectra and the normalized shear modulus  $G/G_0$  for one pass specimen. The excitation frequency,  $f_0 = 4.0$  Hz

### 3.2 Shear modulus in T91 steel

Figure 1(b) shows temperature dependence of the normalized shear modulus,  $G/G_0$ , and internal friction spectra for the 1 pass T91 specimen, where  $G_0$  is the value of the shear modulus measured at room temperature. With increasing temperature the normalized shear modulus  $G/G_0$  shows a descending tendency. When temperature is elevated to about  $707^\circ\text{C}$ , the  $G/G_0$  indicates the minimum value and then turn to a ramping up to a maximum value at around  $745^\circ\text{C}$ . This abnormal change in the  $G/G_0$  does not appear in the cooling curve (or the second heating curve) which the  $G/G_0$  keeps relative higher values only with a monotonic temperature dependence. Dramatic change in the curve of  $G/G_0$  versus temperature denotes the occurrence of a phase transformation or recrystallization, which is also consistent with the non-relaxation behavior of the peak. Similar phenomenon was observed in the ECAP-processed Cu [22,23]. In both cases, the modulus ramp and the abnormal change in the curve of  $G/G_0$  vs. temperature should be associated with the recovery of dislocations and subsequent recrystallization from a severely deformed state. It is worthwhile to note that the start and finish temperature of the recrystallization process. If we presume that the recrystallization began with the

temperature at the turning point in the  $G/G_0$ , namely 707°C, and ended at 745°C, which just correspond to the peak and valley on high-temperature side of the internal friction peak in the first heating run, respectively. Thus, similarly to Al [11], Cu [22,23], and Mg [5], it can be suggested that in the studied steels, the low-temperature side of the peak  $P_1$  may be related to the reversible dislocation movement while the high-temperature side of the peak correlates to an irreversible recrystallization process. This observation underlines common features of loosing thermal stability by various severely deformed metals.

### 3.3 Microstructure analysis

Another issue is whether the abnormal change in the  $G/G_0$  correlates to the grain size variation. Figure 2 shows the TEM images of 4 passes specimens before and after the annealing. For the as-received 4 passes specimen, the average grain size was refined to UFG scale and abundant dislocations were introduced into this specimen, as seen in Fig. 2 (a). After the annealing at 700°C for 1h, the microstructure of grain boundaries and grain interior become clear with a decrease in dislocation density but the average grain size still remains at the UFG level as shown in Fig. 2 (b). This is coinciding with the foregoing internal friction results, namely the low temperature side of the internal friction peak. However, in Fig. 4 (c), no grain boundary is observed in the same observation scale, and the dislocation density is dramatically decreased when the specimen was annealed at 850°C for 1h. It is indicated that the higher annealing temperature leads to the evident grain growth and strain release due to the recrystallization. Therefore, the internal friction peak at the vicinity of 670°C is considered as a microstructural transition from a severely deformed state to a static recovery of dislocations and finally to the recrystallization state. Similar results were reported in ECAP-strained Cu [22,23] and Mg [5].

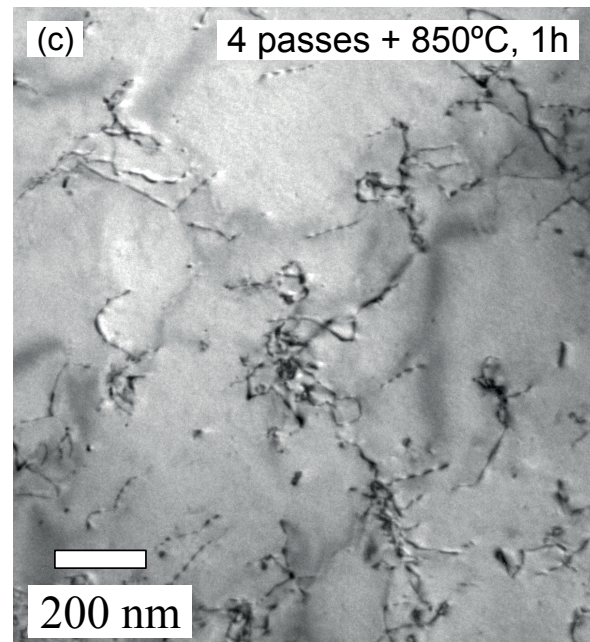
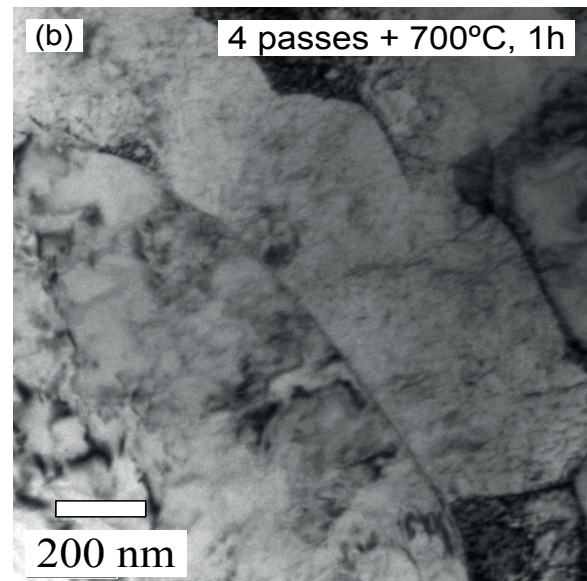
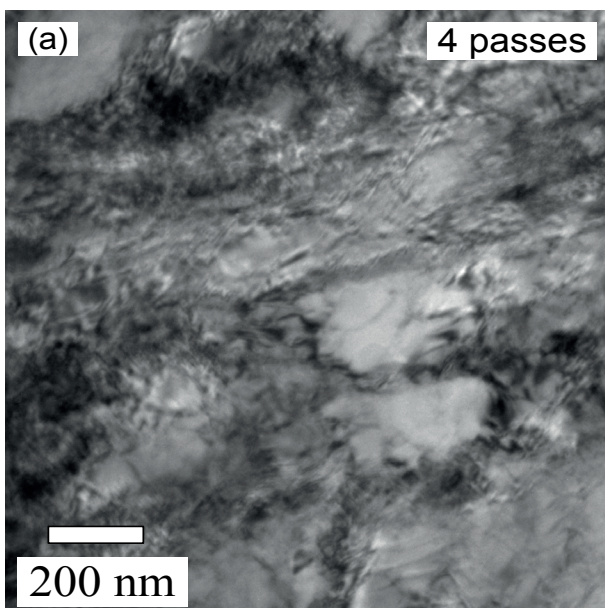


Fig. 2. TEM micrographs for 4 passes T91 specimen (a), 4 passes T91 specimen subjected to annealing at 700°C for 1 h (b) and 850°C for 1 h (c)

### 3.4 Fe-18wt.%Cr steel

The microstructure of T91 steel is complicated. The microstructure is composed of large prior austenitic grains (PAG) with approximately 10  $\mu\text{m}$  in a dimension and martensite laths with a width of about 40 nm inside PAG as reported in our previous paper [21]. Furthermore, large  $\text{M}_{23}\text{C}_6$  carbide particles (100-300 nm) are mainly located along large angle boundaries and smaller MX precipitates (30-50 nm) are distributed rather homogeneously inside the grains [21,24]. It could be speculated that ECAP processing will make the microstructure of T91 steel more complicated (Fig. 2a). To elucidate the nature of the internal friction peak observed at around 670°C, the Fe-18wt.%Cr alloy is selected to study the effect of ECAP processing on internal friction spectra. The Fe-18wt.%Cr alloy is reported to be a pure ferrite phase without carbides (i.e.  $\text{M}_{23}\text{C}_6$  or MX) [25].

Figure 3(a) shows internal friction spectra of the as-received, 1, 2, and 4 passes Fe-18wt.%Cr specimens. No peak is observed in the as-received Fe-18wt.%Cr specimen, like the T91 steel, but there is a peak (referred to as the  $P_1$ ) at 678°C, 666°C and 650°C for 1, 2 and 4 passes specimens, respectively. Similar to T91 steel, the peak temperature of the  $P_1$  shifts toward low temperature with increasing the extrusion number. It reveals a decrease in the thermal stability of the ECAP-strained Fe-18wt.%Cr alloy. The peak temperature of  $P_1$  peak does not depend on the excitation frequency. It is confirmed that the  $P_1$  peak is also a non-relaxation internal friction peak. Figure 3(b) shows internal friction peak and the  $G/G_0$  versus temperature, which are similar to those curves in T91 steel. There is a minimum value on the curve of the  $G/G_0$  at about 678°C, which is corresponding to the peak temperature of the  $P_1$  peak during the first heating. The  $P_1$  peak is also correlated to the microstructural transition from a severely deformed state to a static recovery of dislocations and finally to the recrystallized state.

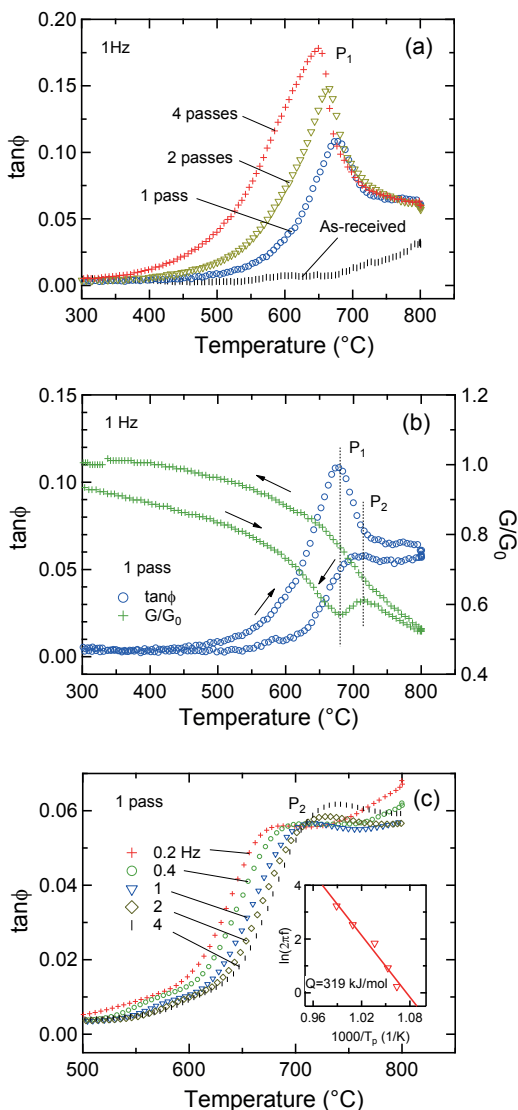


Fig. 3. (a) Internal friction spectra for the as-received Fe-18wt.%Cr alloy, 1 pass, 2 and 4 passes specimens in the first heating run, (b) internal friction spectra and the normalized shear modulus,  $G/G_0$ , for 1 pass specimen in the first heating cooling run, (c) frequency dependence of the  $P_2$  peak; inset: Arrhenius plot for the  $P_2$  peak for 1 pass specimen

### 3.5 Analysis of internal friction and the $P_2$ peak in Fe-18wt.%Cr and T91 steel

Nonetheless, there are two differences in the  $P_1$  peaks observed in ECAP-strained Fe-18wt.% Cr alloy and T91 steel. The height of the  $P_1$  peak increases with increasing the extrusion number for Fe-18wt.% Cr alloy, while it decreases for the T91 steel (Fig. 1(a)). In fact, the same extrusion pass (e.g. 4-pass extrusion) almost results in same level of grain refinement (UFG level) in both T91 steel (Fig. 2a) and Fe-18wt.% Cr steel (not shown here). However, the complicated microstructure of ECAP-strained T91 steel contains more refined carbide particles (e.g.  $M_{23}C_6$ , MX), which may hinder the dislocation multiplication and lead to a reduction in the dislocation density. The height of the  $P_1$  peak could decrease with the number of extrusion pass in T91 steel. The second difference in internal friction spectra between Fe-18wt.%Cr alloy and T91 steel is that it exists the relaxation  $P_2$  peak in the cooling curve and the second heating in the Fe-18wt.%Cr alloy (Fig. 3(b)). The peak  $P_1$  observed in the first heating run should be a sum of the transition peak  $P_1$  and the relaxation peak  $P_2$ . The peak temperatures of  $P_2$  increase with increasing the excitation frequency,  $f$  (Fig. 3(c)). From the inset of Fig. 3(c), the relaxation parameters of the  $P_2$  peak can be estimated as: the activation energy  $H = 319$  kJ/mol and the pre-exponential factor  $\tau_0 = 1.4 \times 10^{-18}$  s. Because the  $\tau_0$  is too small for standard relaxation mechanism induced by point defects, Benoit [26] suggested a grain boundary sliding model and provided a value of the  $\tau_0 = 10^{-15} \times d/\delta$ , where  $d$  is the grain size and  $\delta$  states for the grain boundary width ( $\sim 5$  Å) [26]. If  $d = 500$  nm in this case, the  $\tau_0 = 1 \times 10^{-12}$  s and  $H = 200$  kJ/mol. It is suggested that the  $P_2$  peak may be associated with an impurity impeding grain boundary sliding. The one of reasons is that the evident  $P_2$  relaxation peak appears only in Fe-18wt.% Cr alloy but not in T91 steel. Because more refined carbide particles in T91 steel may act as pinning entities on the grain boundary and then the grain boundary sliding cannot occur.

### 3.6 ECAP-strained tungsten

Figure 4 shows internal friction spectra for the as-received, ECAP-strained W after 1 pass at 800°C and 950°C. Internal friction peaks are observed in the as-received W within the temperature range from 25 to 850°C (Fig. 4(a)). After 1 pass at both 800°C and 950°C, a small internal friction peak is found at about 380°C during the first heating but it disappears during the second heating, as shown in the insets of Figs. 4(b and c). Similar peak was observed at 347-407°C (the excitation frequency, 1-1.3 Hz) in high purity W single crystal after slight plastic deformations at 600 K and at 450 K [27,28]. This peak was defined as the  $\gamma$  peak observed in many bcc metals such as high purity Nb, Ta, Fe, and W. The  $\gamma$  relaxation was attributed to the kink-pair formation on screw dislocations in BCC metals [27]. It should be emphasized that the  $\gamma$  peak appears only in the ECAP-strained W, suggesting that the ECAP processing can produce a lot of mobile screw dislocations. Figure 4(b and c) shows that the  $\gamma$  peak disappears in the second heating. This effect is probably associated with the annihilation and/or bending of screw dislocations [27]. In addition, since the

grain boundary peak in W occurs at around 1730°C [29], it is safe to conclude that the grain boundary peak is not observed in this study.

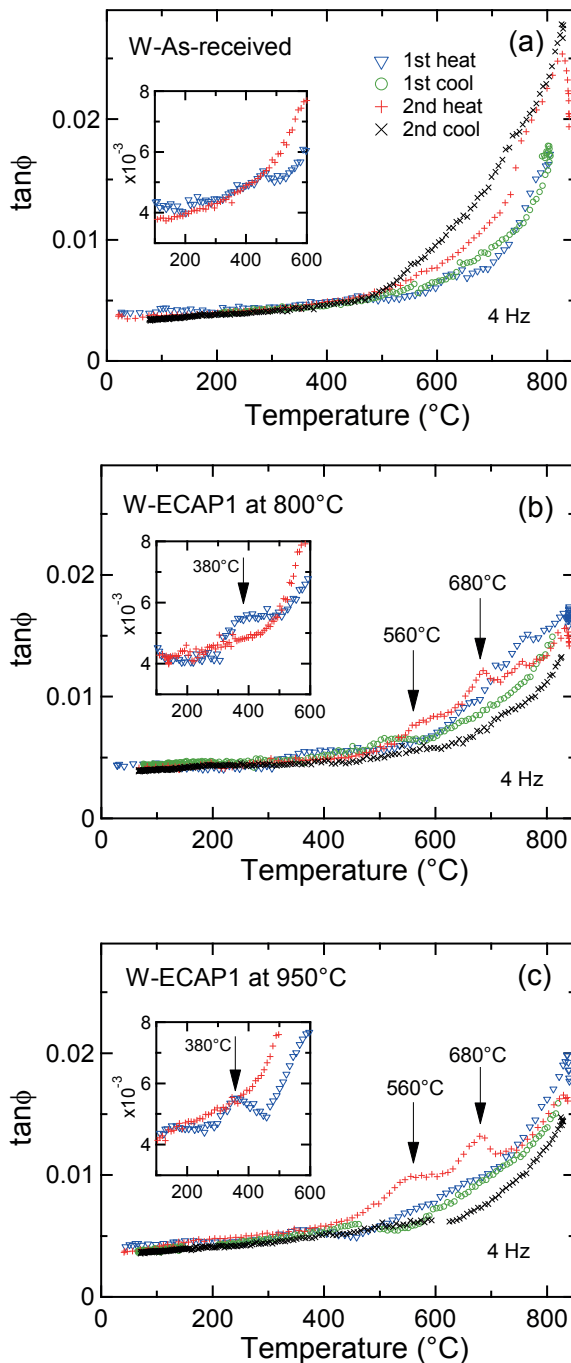


Fig. 4. Internal friction peaks in two heating cooling cycles in: (a) as-received W, (b) 1 pass at 800°C strained W, (c) 1 pass at 950°C strained W; insert: a small peak at 380°C

#### 4. Summary

An asymmetrical non-relaxation internal friction peak  $P_1$  was observed in ECAP-strained ferrite/martensite 9Cr1Mo steel (T91) and ferrite Fe-18wt.%Cr alloy. The  $P_1$  peak

disappears in the second heating run, indicating that severely deformed materials are thermally unstable in the studied temperature range. The abnormal variation of the normalized shear modulus,  $G/G_0$ , was found in both ECAP-strained T91 steel and Fe-18wt.% Cr alloy. It is suggested that the  $P_1$  peak consists of two physical processes: one is related to the recovery process of dislocations on the low-temperature side of the  $P_1$  peak and the another process corresponds to the recrystallization on the high-temperature side of the  $P_1$  peak. We also underline that such a phenomenon is typical not only for ECAP-strained steels but also for ECAP-strained Al, Cu, and Mg.

The relaxation peak  $P_2$  in Fe-18wt.%Cr alloy was observed during the first cooling and second heating runs. The  $P_2$  peak is considered as a grain boundary sliding peak. A number of  $M_{23}C_6$  carbides distributed along grain boundaries and martensite lath boundaries may act as pinning entities on grain boundary to impede their sliding. Thus, the  $P_2$  peak was not detected in ECAP-strained T91. A small internal friction peak at around 380°C is observed in the first heating run in ECAP-strained W. The 380°C peak is accounted for in terms of the  $\gamma$  internal friction peak observed in deformed BCC metals.

#### Acknowledgements

This work was financially supported by the National Natural Science Foundation of China (Grant No. 11374299 and No. 051071148.)

#### REFERENCES

- [1] R. Saha, R. Ueji, N. Tsuji, Fully recrystallized nanostructure fabricated without severe plastic deformation in high-Mn austenitic steel, *Scripta Mater.* **68**, 813-816 (2013).
- [2] Y. Estrin, A. Vinogradov, Extreme grain refinement by severe plastic deformation: A wealth of challenging science, *Acta Mater.* **61**, 782-817 (2013).
- [3] R.Z. Valiev, T.G. Langdon, Principles of equal-channel angular pressing as a processing tool for grain refinement, *Prog. Mater. Sci.* **51**, 881-981 (2006).
- [4] S. Komura, Z. Horita, M. Nemoto, T.G. Langdon, Influence of stacking fault energy on microstructural development in equal-channel angular pressing, *J. Mater. Res.* **14**, 4044-4050 (1999).
- [5] G.D. Fan, M.Y. Zheng, X.S. Hu, C. Xu, K. Wu, I.S. Golovin, Improved mechanical property and internal friction of pure Mg processed by ECAP, *Mater. Sci. Eng. A* **556**, 588-594 (2012).
- [6] M. Suś-Ryszkowska, T. Wejrzanowski, Z. Pakieła, K. Kurzydłowski, Microstructure of ECAP severely deformed iron and its mechanical properties, *Mater. Sci. Eng. A* **369**, 151-156 (2004).
- [7] Y. Zhang, A.V. Ganeev, J.T. Wang, J.Q. Liu, I.V. Alexandrov, Observations on the ductile-to-brittle transition in ultrafine-grained tungsten of commercial purity, *Mater. Sci. Eng. A* **503**, 37-40 (2009).
- [8] Y.H. Zhao, X.Z. Liao, Z. Jin, R.Z. Valiev, Y.T. Zhu, Microstructures and mechanical properties of ultrafine grained 7075 Al alloy processed by ECAP and their evolutions during

- annealing, *Acta Mater.* **52**, 4589-4599 (2004).
- [9] Y. Fukuda, K. Oh-Ishi, Z. Horita, T. Langdon, Processing of a low-carbon steel by equal-channel angular pressing, *Acta Mater.* **50**, 1359-1368 (2002).
- [10] M. Eddahbi, M.A. Monge, T. Leguey, P. Fernández, R. Pareja, Texture and mechanical properties of EUROFER 97 steel processed by ECAP, *Mater. Sci. Eng. A* **528**, 5927-5934 (2011).
- [11] I.S. Glovin, A.V. Mikhaylovskaya, H.R. Sinning, Role of the b-phase in grain boundary and dislocation anelasticity in binary Al-Mg alloys, *J. Alloy Compd.* **577**, 622-632 (2013).
- [12] A.S. Nowick, B.S. Berry, *Anelastic Relaxation in Crystalline Solids*, Academic Press, New York, (1972).
- [13] R. de Batist, *Internal Friction of Structural Defects in Crystalline Solids*, North-Holland Publishing Company, (1972).
- [14] T.S. Kê, *Internal Friction Theory in Solids*, Science Press, Beijing, (2000).
- [15] L.B. Magalas, *Mechanical spectroscopy – Fundamentals*, *Sol. St. Phen.* **89**, 1-22 (2003).
- [16] S. Etienne, S. Elkoun, L. David, L.B. Magalas, *Mechanical spectroscopy and other relaxation spectroscopies*, *Sol. St. Phen.* **89**, 31-66 (2003).
- [17] M.S. Blanter, I.S. Golovin, H. Neuhauser, H.R. Sinning, *Internal Friction in Metallic Materials: A Handbook*, Springer, (2007).
- [18] L.B. Magalas, *Mechanical spectroscopy, internal friction and ultrasonic attenuation. Collection of works*, *Mater. Sci. Eng. A*, **521-522**, 405-415 (2009).
- [19] Q.F. Fang, X.P. Wang, X.B. Wu, H. Lu, The basic principles and applications of internal friction and mechanical spectroscopy, *Physics* **40**, 786-793 (2011).
- [20] T. Hao, Z.Q. Fan, S.X. Zhao, G.N. Luo, C.S. Liu, Q.F. Fang, Microstructures and properties of ultrafine-grained tungsten produced by equal-channel angular pressing at low temperatures, *J. Nucl. Mater.* **433**, 351-356 (2013).
- [21] T. Hao, Z.Q. Fan, S.X. Zhao, G.N. Luo, C.S. Liu, Q.F. Fang, Strengthening mechanism and thermal stability of severely deformed ferritic/martensitic steel, *Mater. Sci. Eng. A* **596**, 244-249 (2014).
- [22] I.S. Golovin, P. Pal-Val, L. Pal-Val, E. Vatazhuk, Y. Estrin, The effect of annealing on the internal friction in ECAP-modified ultrafine grained copper, *Sol. St. Phen.* **184**, 289-294 (2012).
- [23] N. Kobelev, E. Kolyvanov, Y. Estrin, Temperature dependence of sound attenuation and shear modulus of ultra fine grained copper produced by equal channel angular pressing, *Acta Mater.* **56**, 1473-1481 (2008).
- [24] B. Fournier, M. Sauzay, A. Pineau, Micromechanical model of the high temperature cyclic behavior of 9-12% Cr martensitic steels, *Int. J. Plast.* **27**, 1803-1816 (2011).
- [25] Y.V. Konobeev, A.M. Dvoriashin, S.I. Porollo, F.A. Garner, Swelling and microstructure of pure Fe and Fe-Cr alloys after neutron irradiation to ~26 dpa at 400°C, *J. Nucl. Mater.* **355**, 124-130 (2006).
- [26] W. Benoit, High-temperature relaxations, *Mater. Sci. Eng. A* **370**, 12-20 (2004).
- [27] U. Ziebart, H. Schultz, Dislocation relaxation peaks in high purity tungsten single crystals, *J. de Phys.* **44** (C9), 691-696 (1983).
- [28] H. Schultz, G. Funk, U. Ziebart, R. Bauer, The intrinsic dislocation relaxation spectrum of niobium, tantalum and tungsten, *J. de Phys.* **46** (C10), 289-292 (1985).
- [29] I. Berlec, The effects of impurities and heat treatment on the internal friction of tungsten at high temperatures, *Metall. Trans.* **1**, 2677-2683 (1970).